

The complex permittivity of the material is then obtained by means of the program presented in [3]. By including in the computer procedure the search for  $\alpha$  and  $\beta$ , one would be able to determine  $\epsilon_r$  directly from the slotted line measurements (location and amplitude of the extrema). This technique, however, remains limited to those situations where the standing-wave pattern presents extrema; this is no longer the case for highly lossy materials or far from the shorted termination.

The method presented here can readily be used in other situations where the propagation coefficient is to be determined from field pattern measurements along open lines: microstrip, microslot, dielectric waveguides, G-lines, and confocal transmission lines, to name only a few.

## REFERENCES

- [1] P. Bhartia and M. A. K. Hamid, "Dielectric measurements of sheet materials," *IEEE Trans. Instrum. Meas.* (Short Papers), vol. IM-22, pp. 94-95, Mar. 1973.
- [2] I. J. Bahl and H. M. Gupta, "Microwave measurement of dielectric constant of liquids and solids using partially loaded slotted waveguide," *IEEE Trans. Microwave Theory Tech.* (Short Papers), vol. MTT-22, pp. 52-54, Jan. 1974.
- [3] P. I. Somlo, "The exact numerical evaluation of the complex dielectric constant of a dielectric partially filling a waveguide," *IEEE Trans. Microwave Theory Tech. (Lett.)*, vol. MTT-22, pp. 468-469, Apr. 1974.
- [4] E. Lertes and R. Kaminski, "Zur bestimmung der komplexen Dielektrizitätskonstante von Flüssigkeiten in Koaxialleitern mittels Abtastung des stehenden Wellenfeldes innerhalb der Probe," *Arch. Tech. Mes. Ind. Messtech.*, vol. V, p. 13, Dec. 1973.
- [5] J. W. Bandler and P. A. MacDonald, "Optimization of microwave networks by razor search," *IEEE Trans. Microwave Theory Tech. (Special Issue on Computer-Oriented Microwave Practices)*, vol. MTT-17, pp. 552-562, Aug. 1969.

## Measurement of the Electromagnetic-Field Components in a Rectangular Drift Tube-Loaded Cavity Using Various Perturbing Objects

F. BRUNNER, W. SCHOTT, AND H. DANIEL

**Abstract**—The electric-field quantities  $E$ ,  $E_y$ ,  $E_z$ , and the magnetic-field quantities  $H$  and  $H_z$  in a rectangular drift tube-loaded cavity resonating in the  $TE_{101}$  mode have been measured along the  $z$  direction by means of the perturbation method using a dielectric bead, a metallic disk, a metallic needle, a metallic sphere, and a ferrite disk. The relative errors for  $E$  and  $E_y$  are 3 percent; for  $E_z$ , 10 percent on the average; whereas for  $H$  and  $H_z$ , they are 10 percent at least. The ferrite disk, being superior to the metallic sphere, offers a new technique in determining magnetic-field components in cavity resonators.

## I. INTRODUCTION

The fields in the second half of a rectangular cavity resonator operating in the  $TE_{101}$  mode can be used for the phase-free acceleration of charged particles, i.e., no fixed phase relation between the phases of entrance of the particles into the fields and the phases of the fields is necessary for the acceleration [1]. In Fig. 1 a cavity resonator of this type is sketched. The reference axis for the particles is a straight line at  $x = a/2$ ,  $y = b/2$  parallel to the  $z$  axis. There is a beam hole of 4-cm diameter at the front and rear plate of the resonator. The fields in the first half of the resonator are shielded by a drift tube of length  $d/2$  and 4-cm diameter which is mounted at the front plate. In order to be able to calculate particle trajectories and the energy gain within the resonator, the electric and magnetic fields must be known fairly accurately in the plane  $x = a/2$  around the reference axis. Using the perturbation technique, field measurements on the reference axis and on an axis at a distance of 1 cm parallel to the reference axis in the  $x = a/2$  plane were made.

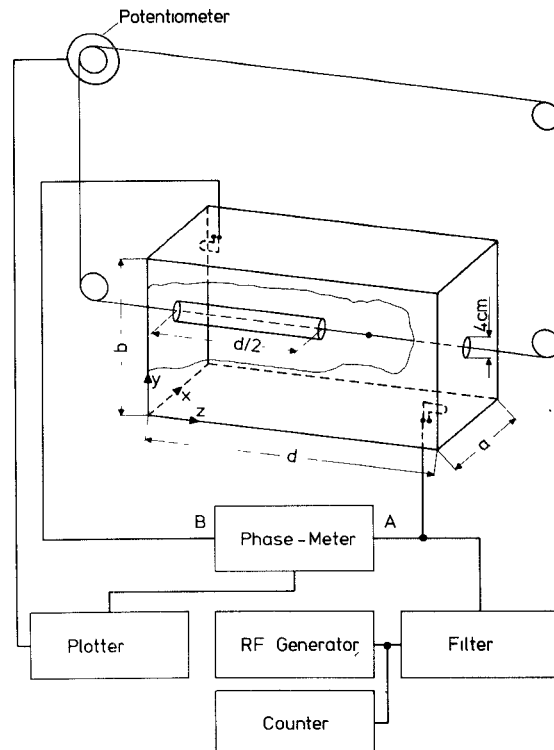


Fig. 1. Experimental setup for measuring the electromagnetic fields of a drift tube-loaded cavity resonator. The dimensions of the resonator were chosen to be  $a = 25.4$ ,  $b = 30.0$ , and  $d = 55.3$  cm. The drift tube has a diameter of 4 cm.

## II. EXPERIMENTAL

The experimental setup is shown schematically in Fig. 1. The general perturbation method was described already by Hansen and Post [2]. Special techniques for measuring small frequency shifts in cavities were reported, e.g., by Hahn and Halama [3]. The relative frequency shift  $\delta\omega/\omega$  which is caused by the perturbing object is obtained from the phase difference  $\delta\phi$  between the input and output signal of the resonator by

$$\delta\omega/\omega = \delta\phi/2Q \quad (1)$$

where  $Q$  is the  $Q$  factor of the resonator. The linear relation between  $\delta\phi$  and  $\delta\omega/\omega$  is fulfilled within better than 1 percent if  $\delta\phi$  is less than  $10^\circ$ . With the resonance frequency  $\nu = 639.44$  MHz, the experimental  $Q$  factor  $Q = 4388$ , and choosing the size of the perturbing object in such a way that  $\delta\phi_{\max} \approx 6^\circ$ , we got for the maximum frequency shift  $(\delta\omega/\omega)_{\max} \approx 1.2 \cdot 10^{-5}$ . Measurements of such small frequency shifts require short measuring times to avoid a drift of the resonant frequency of the system. Therefore, a time of 1.5 min was chosen during which the perturbing object was pulled through the resonator by the pulley system. Moreover, the RF generator was quartz stabilized within 1 Hz. The position  $z$  of the perturbing object and the phase difference  $\delta\phi$  were recorded by a plotter. The frequency shifts caused by ellipsoid-shaped perturbation objects are calculated and extensively reviewed in a paper by Voisin [4]. The frequency shift  $(\delta\omega/\omega)_i$  caused by a special object  $i$  can be written

$$\left( \frac{\delta\omega}{\omega} \right)_i = -\pi R_i^3 \omega \left[ \epsilon_0 \left( F_{||i}(\epsilon_r, \beta_i) \frac{E_{||i}^2}{PQ} + F_{\perp i}(\epsilon_r, \beta_i) \frac{E_{\perp i}^2}{PQ} \right) + \mu_0 \left( G_{||i}(\mu_r, \beta_i) \frac{H_{||i}^2}{PQ} + G_{\perp i}(\mu_r, \beta_i) \frac{H_{\perp i}^2}{PQ} \right) \right] \quad (2)$$

where  $\beta_i = a_i/R_i$  is the ratio of the shorter to the longer semiaxis of the ellipsoid, and  $F_{||i}$ ,  $F_{\perp i}$ ,  $G_{||i}$ , and  $G_{\perp i}$  are functions depending on the shape, the permittivity, and the permeability of the perturbing object.  $E_{||i}$ ,  $E_{\perp i}$ ,  $H_{||i}$ , and  $H_{\perp i}$  are the electric- and magnetic-field

TABLE I

i	2R (mm)	2a (mm)	$\beta = a/R$	$\epsilon_r$	$\mu_r$	$F_{  }$	$F_{\perp}$	$G_{  }$	$G_{\perp}$
1 (= Cu-disk)	7	0.1	0.014			0.424	$4.77 \cdot 10^{-3}$	$4.72 \cdot 10^{-3}$	0.424
2 (= Ag-bead)	5					1	1	0.5	0.5
3 (= teflon bead)	8			2.03	1	0.256	0.256		
4 (= ferrite disk)	8	0.8	0.1	12.13	10.0	0.209	0.035	0.184	0.034
5 (= steel needle)	9.1	0.2	0.022			0.0945	$3.232 \cdot 10^{-4}$	$1.616 \cdot 10^{-4}$	$3.220 \cdot 10^{-4}$

components parallel and perpendicular to the larger semiaxis of the ellipsoid, respectively. In Table I, the dimensions, the permittivity, the permeability of the used perturbing objects, and the functions  $F_{||}, \dots, G_{\perp}$  are listed. The permittivities of the Teflon bead and the ferrite disk were measured using the cavity resonator with the drift tube removed. In an ideal resonator of this type, there are only  $E_y$ - and  $H_x$ -field components in the plane  $x = a/2$ . At  $x = a/2, y = b/2$ , and  $z = d/2$  the component  $E_y$  has a maximum. There, deviations from the ideal field caused by the beam holes are negligible, and one has  $E_y/(PQ)^{1/2} = (8/\epsilon_0\omega abd)^{1/2}$  and  $H_x$  is zero. Thus  $\epsilon_r$  can be determined for a specimen brought to that point measuring  $\delta\omega/\omega$  and using (2).

### III. RESULTS AND DISCUSSION

It can be deduced from Table I that the components  $E_y/(PQ)^{1/2}$  and  $E_z/(PQ)^{1/2}$  are obtained directly from the metal disk and the metal needle measurements. For reasons of symmetry the field components  $E_x, H_y$ , and  $H_z$  vanish in the plane  $x = a/2$ . Using the Teflon bead, the absolute value of the electric field  $E/(PQ)^{1/2}$  is obtained. Furthermore, the metal disk and the steel needle measurements are combined to values of  $E/(PQ)^{1/2}$  by  $E/(PQ)^{1/2} = (E_y^2/PQ + E_z^2/PQ)^{1/2}$ . The Teflon bead and the steel needle measurements give further  $E_y/(PQ)^{1/2}$  values by  $E_y/(PQ)^{1/2} = (E^2/PQ - E_z^2/PQ)^{1/2}$ . Finally, the Teflon bead and the metal disk measurements yield values of  $E_z/(PQ)^{1/2}$  by  $E_z/(PQ)^{1/2} = (E^2/PQ - E_y^2/PQ)^{1/2}$ . Fig. 2 shows the results of the absolute value of the electric field, the electric-field components  $E_y$  and  $E_z$ , and the magnetic-field component  $H_x$  measured on the two axes parallel to the  $z$  axis at  $y = b/2$  and  $y = b/2 - 1$  cm in the  $x = a/2$  plane. Concerning the electric fields, the full lines represent the directly measured fields, whereas the values, which were combined by two measurements, are marked by circles. Both results agree well. The relative errors for determining  $E/(PQ)^{1/2}$  and  $E_y/(PQ)^{1/2}$  are about 3 percent, as indicated in Fig. 2, for the  $E_y/(PQ)^{1/2}$  curve at  $y = b/2$ .

$E_z/(PQ)^{1/2}$  was obtained within 10 percent as shown for  $y = b/2 - 1$  cm.  $E_z$  vanishes on the axis  $y = b/2$  within the limits of error.

The magnetic field is more difficult to measure in our case because it has a much smaller effect on  $\delta\omega/\omega$  than the electric field. The ratio of the maximum values of  $\mu_0 H_x^2/PQ$  and  $\epsilon_0 E_y^2/PQ$ , e.g.,

$$\left( \frac{\mu_0 H_x^2}{\epsilon_0 E_y^2} \right)_{TE_{101}} = \frac{\pi^2 c^2}{\omega^2 d^2}$$

is only 0.17, assuming an ideal field distribution. In order to determine  $H/(PQ)^{1/2}$  and  $H_z/(PQ)^{1/2}$ —both values should be identical here—we used a dielectric and a metallic sphere in the first case, and a dielectric sphere, a ferrite disk, and a metallic needle in the second case. The metallic needle data are necessary only for  $y = b/2 - 1$  cm where  $E_z$  is different from zero. The use of a ferrite perturbing object is a new technique. The quotient of the perturbing object function  $G$  of the magnetic-field term in (2), divided by the function  $F$  of the electric-field term (cf. Table I), is nearly twice as large for the ferrite disk as for the metallic sphere. This gives a better accuracy of the magnetic-field measurement using the ferrite disk than using the metallic sphere in regions where the electric fields are not too large, i.e., near the end of the drift tube and for

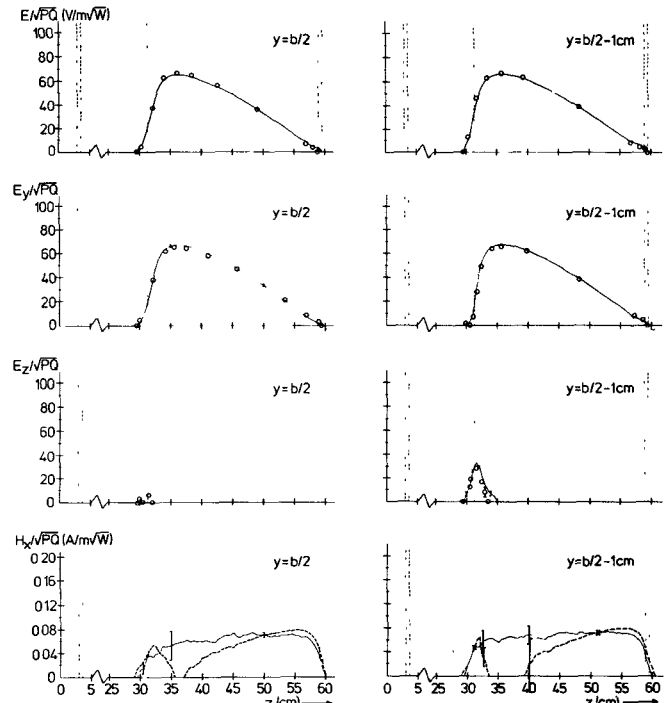


Fig. 2. Results of perturbation-object measurements  $E, E_y, E_z, H$ , and  $H_x$  versus the  $z$  coordinate of the resonator at  $y = b/2$  and  $y = b/2 - 1$  cm in the plane  $x = a/2$ . In the case of the electric fields, the drawn lines represent direct measurements. The used perturbing objects were a Teflon sphere for  $E/(PQ)^{1/2}$ , a metallic disk for  $E_y/(PQ)^{1/2}$ , and a metallic needle for  $E_z/(PQ)^{1/2}$ . The circles represent values which were composed from different measurements.  $E/(PQ)^{1/2} = (E_y^2/PQ + E_z^2/PQ)^{1/2}$ ,  $E_y/(PQ)^{1/2} = (E^2/PQ - E_z^2/PQ)^{1/2}$ , and  $E_z/(PQ)^{1/2} = (E^2/PQ - E_y^2/PQ)^{1/2}$ . In the case of the magnetic field, the drawn lines reproduce measurements of  $H/(PQ)^{1/2}$  where a Teflon sphere and a metallic sphere were used. The dotted lines are values of  $H_x/(PQ)^{1/2}$  which were obtained by a Teflon bead, a ferrite disk, and a metallic needle.  $P$  is the power loss and  $Q$  is the  $Q$  factor of the resonator. The double dotted lines represent the front and rear plates; the single dotted lines represent the middle of the cavity.

$z \geq 50$  cm. The results of  $H/(PQ)^{1/2}$  are drawn as full lines in Fig. 2. The dotted lines represent the  $H_x/(PQ)^{1/2}$  values. As can be seen from the graph for  $y = b/2 - 1$  cm, the errors of the dotted line are slightly smaller and the curve itself is smoother than the full line in the previously mentioned regions. However, the relative errors are 10 percent at least. In the region where  $E_y/(PQ)^{1/2}$  is large, both methods for determining  $H/(PQ)^{1/2}$  and  $H_z/(PQ)^{1/2}$  become very inaccurate. Nevertheless, a decrease of the magnetic field in that region and an increase close to the end of the drift tube are obvious, as can be seen from the ferrite-disk measurements for both  $y$  values.

### REFERENCES

- [1] W. Schott *et al.*, in *Proc. 9th Int. Conf. High Energy Accelerators* (Stanford, Calif., 1974), to be published.
- [2] W. W. Hansen and R. F. Post, *J. Appl. Phys.*, vol. 19, p. 1059, 1948.
- [3] H. H. Hahn and H. J. Halama, "Perturbation measurement of transverse R/Q in iris-loaded waveguides," *IEEE Trans. Microwave Theory Tech.*, vol. MTT-16, pp. 20-29, Jan. 1968.
- [4] G. Voisin, "Application de la méthode des perturbations à la mesure du champ électromagnétique dans de cavités résonnantes," M.S. thesis, University of Lyons, Lyons, France, 1966.